Polymer Composites

WILEY | spe INSPIRING PLASTICS PROFESSIONALS

RESEARCH ARTICLE

Influence of Residual Stresses in CF/PEEK Tape and Heating Methods on Deconsolidation Behavior During the Heating Phase of Laser-Assisted Automated Fiber Placement

Qiuyu Miao[1,2] | Daniël Peeters[1] | Dongjiang Wu[2] | Julie Teuwen[1]

[1]Aerospace Structures and Materials, Faculty of Aerospace Engineering, Delft University of Technology, Delft, the Netherlands | [2]State Key Laboratory of High-Performance Precision Manufacturing, Dalian University of Technology, Dalian, China

Correspondence: Qiuyu Miao (qymiao@nuaa.edu.cn)

Received: 3 September 2025 | **Revised:** 25 October 2025 | **Accepted:** 12 November 2025

Keywords: deconsolidation behavior | interlaminar voids | laser-assisted automated fiber placement (LAFP) | residual stress | thermoplastic (TP) tape

ABSTRACT

The high void content in laser-assisted fiber placement (LAFP)-manufactured thermoplastic (TP) hinders industrial adoption, with tape deconsolidation being a critical yet understudied factor. To address this research gap, this study provides an in-depth investigation into the deconsolidation mechanisms of TP tapes during the LAFP heating phase. A series of comparative experiments were conducted to systematically evaluate the effects of tape residual stress states (fiber-matrix combined, fiber-dominated, and near stress-free) and heating methods (laser vs. oven heating) on deconsolidation behavior. Deformation along the width, voids, thickness variations and surface roughness were identified as key factors to characterize deconsolidation behavior and to elucidate its underlying mechanisms. The results reveal that the matrix residual stress plays a dominant role in exacerbating deformation along the width, nonuniformity in thickness and intralaminar voids. Additionally, fiber decompaction—induced by the recovery of elastic deformation—contributes to surface deformation by generating voids near the surfaces. Furthermore, laser-heated tapes exhibit more pronounced intralaminar voids and higher surface roughness than oven-heated counterparts, underscoring the influence of heating rate on the release of residual stress. This study advances the understanding of deconsolidation mechanisms during the LAFP heating phase, and provides recommendations for optimizing the manufacturing of LAFP-grade TP tapes.

1 | Introduction

Thermoplastic (TP) composites, with the ability to be repeatedly melted and consolidated, are often subjected to (re-)heating/cooling processes to form a complex shaped component from laminates [1, 2], and/or to join parts [3, 4]. It is reported that when TP laminates are heated without pressure, the laminates deconsolidate, causing for instance voids as a defect [5, 6], which are unfavorable to the quality of the final product, as they can reduce the mechanical properties of TP components [7].

During automated fiber placement (AFP) of TP composites, the absence of pressure on TP tapes during the heating phase leads to deconsolidation [8, 9]. Kok [9] captured the deconsolidated tapes by using a steel tool to freeze the tape after being heated, showing intralaminar voids, a rough and matrix-poor surface, which could hinder the development of intimate contact, crucial for bond quality between TP layers [10]. Therefore, understanding the main mechanisms of deconsolidation is important to minimize its occurrence and thereby improve the interlaminar bonding quality of TP composites manufactured by AFP [8].

Highlights

- Decoupling tape residual stresses to access deconsolidation mechanisms.
- Laser-deconsolidated tapes show intensified deconsolidation behavior.
- Matrix residual stress triggers deformation, thickness variation, and intralaminar voids.
- Fiber decompaction generates the formation of voids near surfaces.
- This work provides recommendations for the manufacturing of LAFP-grade TP tapes.

Deconsolidation experiments of TP tapes/laminates were conducted to understand the deconsolidation behavior by heating them to a high temperature (higher than the melting temperature) without pressure and with a dwell for several minutes, which makes it possible to characterize the deconsolidation behavior through in situ and ex-situ measurements. Moisture is considered one of the main reasons for the deconsolidation behavior of TP laminates, which significantly influences the interlaminar bonding but has minimal impact on intralaminar regions [11, 12]. The thermal expansion of dissolved moisture contributes to the laminate deconsolidation as deconsolidation was observed in laminates with moisture and no deconsolidation in laminates dried through heat treatment (250°C for 3 h). But since the residual stress cannot remain the same during the drying process (especially when the temperature is above the glass transition temperature of the matrix), it is impossible to completely distinguish between the suppression of deconsolidation behavior by the removed moisture and by the relaxed residual stress. According to Slange's work [13] on the deconsolidation behavior of TP tapes, it is found that tapes produced by different manufacturers, with the same main specifications such as fiber volume fraction and thickness, exhibit different deconsolidation behavior (all heated in an oven at 390°C for 20 min without pressure). It indicates that the possible different residual stresses in TP tapes generated in different tape manufacturing processes could play an important role in the deconsolidation behavior.

There could be three sources of residual stress within unidirectional TP tapes: residual stress from fibers, matrix and fiber/matrix interface, which are developed during the tape manufacturing process. During the tape manufacturing process, the pulling force on the fibers, which enables their spreading and impregnation, causes elastic deformation of the fibers that is frozen in the form of residual fiber stress after the manufacturing process [14]. The residual stress may also develop in the matrix, as molecular chains would orient along the force direction of squeeze rollers, putting them in a high potential energy state (unstable condition) while they do not have enough time to relax due to the high cooling rate of the process (melt impregnation) [14]. Besides, the crystallization of the matrix during the cooling phase of the tape manufacturing process also increases the residual stress because of the shrinkage when the matrix changes from amorphous state to crystalline state [15, 16]. The last type of residual stress is at the fiber-matrix interface and is caused by the coefficient of thermal expansion (CTE) mismatch between the fiber and the matrix when cooling, which makes the fibers subjected to compressive stress and the matrix subjected to tensile stress upon cooling [17]. Besides, the crystallization of the matrix can also increase the interfacial residual stress.

Slange et al. [11] studied the influence of the residual stress within CF/PEEK tapes on deconsolidation behavior. Two groups of experiments were conducted, one group of tapes press-consolidated at 386°C (above T_m) and 10 bar for 20 min followed by a cooling process with a rate of 2.5°C/min to relax residual stresses in the tape, another group heat-treated at 250°C (above T_g, below T_m) for 3 h to only relax matrix residual stress in the tape. The press-consolidated tapes did not deconsolidate after being reheated to 390°C in the oven, while the heat-treated tapes deconsolidated, which proves the residual stress in the tape plays a role in the deconsolidation behavior. However, it remains unclear which kind of residual stress predominantly influences the deconsolidation process, as the relaxation of matrix residual stress in the CF/PEEK tape may be incomplete after being annealed at 250°C for only 3 h. The remaining matrix residual stress could also cause deconsolidation behavior. This is proved by another study where $[-45/90/45/0]_{3s}$ CF/PEKK laminates manufactured by autoclave, were then annealed at 240°C for 6 h and still exhibited deconsolidation when reheated to 410°C in an oven, while no deconsolidation was observed after being annealed at 240°C for 20 h. This indicates that there is remaining residual stress in the laminate after being annealed for 6 h [5]. Additionally, reported literature mainly focused on tape deconsolidation behavior for slow heating rates (oven heating), while this does not represent the very fast heating rate tapes experienced in LAFP.

In this paper, we aim to investigate the effect of residual stress types in CF/PEEK tapes on deconsolidation behavior under LAFP process conditions. We mainly focused on the fiber residual stress and matrix residual stress in this work. We attempted to decouple residual stresses of fibers and matrix of the tape by oven consolidation, to study their influence on tape deconsolidation. Since residual stress at the fiber–matrix interface is always present in all tapes manufactured in this study, its influence on deconsolidation behavior is considered a constant background effect. These fiber–matrix interface residual stresses could result from for instance different coefficients of thermal expansion (CTE) between the fiber and matrix, as well as matrix crystallization.

The oven consolidation experiments in this work were designed to get three groups of tapes: (1) tapes with both fibers and matrix residual stresses (as-received) (FMS), (2) tapes with only fibers residual stress (FS), and (3) tapes without residual stress (NS). Subsequently, deconsolidation experiments were carried out by heating the tapes using either a convection oven or a laser to analyze the deconsolidation behavior. The deformation along the width, thickness, voids, and surface roughness of the tapes was characterized to understand the deconsolidation behavior.

2 | Materials and Methods

2.1 | Experiments of Decoupling Residual Stresses in Tapes

The CF/PEEK tapes used in this work were supplied by Toray Advanced Composites and manufactured by solvent process. The material properties provided by the manufacturer [18] are listed in Table 1. The as-received tape is referred to as FMS tape (short for "Fiber and Matrix residual stresses").

To get CF/PEEK tapes with different residual stress levels, oven consolidation treatments were carried out (Table 2). First, tapes assumed without residual stress were obtained by heating them while applying pressure in a convection oven (Figure 1a). CF/PEEK tapes, with a length of 100 mm and a width of 6.35 mm, were placed 10 mm apart between two steel plates (coated with release agent). Each group has three or more tapes. In this experiment, pressures of 0.2, 0.4, 0.6, and 0.9 bar by placing weights on top of the upper steel plate, were applied to determine the minimum pressure required to prevent the tapes from deconsolidating during their oven heating. The temperature was measured by K-type thermocouples (with a diameter of 0.7 mm) fixed on top of the tapes. FMS tapes were heated to 390°C at around 2.5°C/min and held for 30 min in the oven, and cooled down in the oven through natural convection. Due to the slow cooling rate (around 1.7°C/min), it is assumed that there is almost no residual stress in the tapes after oven consolidation, referred to as NS tapes (short for "No residual Stress").

TABLE 1 | Material properties of CF/PEEK tape used in this work [17].

Physical properties	Value
Glass transition temperature T_g (°C)	143
Melting temperature T_m (°C)	343
Matrix mass fraction	34%
Thickness (mm)	0.14

TABLE 2 | Heat treatment parameters for all three groups of tapes.

Sample	Sample description	Heat treatment conditions
FMS tape	As-received tape, with both fiber and matrix residual stresses	/
FS tape	Heat-treated tape, with significant fiber residual stress	10 N tape tension was applied. Heated to 390°C at around 2.5°C/min and held for 30 min, and then cooled down in the oven through natural convection
NS tape	Heat-treated tape, with no significant residual stress	Heated to 390°C at around 2.5°C/min and held for 30 min, under a pressure of 0.2, 0.4, 0.6, or 0.9 bar, and cooled down in the oven through natural convection

Second, to get CF/PEEK tapes with only fiber residual stress, named FS tapes, an experimental setup was designed to apply 10 N tape tension, as depicted in Figure 1b. Tapes were placed on top of a C-shaped tool. The pressure P generated by the tape tension on the tape at the corners of the tool can be determined using Equation (1) [19]:

$$P = \frac{F}{wR} \tag{1}$$

in which F is the tape tension (10 N), w is the tape width, and R is the radius of the corner (approximately 35.18 ± 1.90 mm, measured by image software). The pressure P was determined to be 0.45 ± 0.03 bar. The heat treatment applied to the tapes in the oven is the same as for the NS tapes. Due to the application of tension on the fibers during heating and cooling, tapes with only fibers residual stress can be obtained. In the corner areas, fibers' residual stress is not only from tape tension but also the compressive stress from the tool (as shown in the dashed box in Figure 1b), which is similar to the stress conditions of the fibers during the tape manufacturing process. The parts of the tape at the corners (indicated by the solid box in Figure 1b), were cut to study the deconsolidation behavior. Therefore, this group of tapes is shorter, with a length of around 30 mm (around 10 mm for the curved part and 20 mm for the flat part) and have a slight curvature.

2.2 | Deconsolidation Experiments

Two deconsolidation methods, oven deconsolidation and laser deconsolidation, were used to understand potential differences in the deconsolidation mechanisms of the tapes in processes with slow and fast heating rates. During oven deconsolidation, tapes were heated to 390°C and then held for 40 min, after which they were cooled down to room temperature through natural convection in the oven.

The laser deconsolidation experiments utilized a TRUMPF PPM411-12-980-24 VCSEL (Vertical-Cavity Surface-Emitting Laser) heater with a total output capacity of 2.4 kW and a wavelength of 980 nm. The settings of the laser were chosen to reach the target temperature of 390°C: 11 of the 12 heating zones were used, at a power of 890 W, with a heating time of 800 ms, representative of in situ consolidation settings. The heated length was chosen as 65 mm. The temperature history and surface profiles of tapes were recorded during the heating and subsequent cooling process, using a FLIR long wave infrared (LWIR) camera (sampling rate of 50 Hz and resolution of 640×840 pixels) and a Micro-Epsilon scan-CONTROL 2950-25 laser line scanner (LLS) with a sampling rate of 100 Hz, mounted at an angle of around 15°. Figure 1c illustrates the experimental setup of laser deconsolidation. The tape was fixed and lifted up around 5 mm

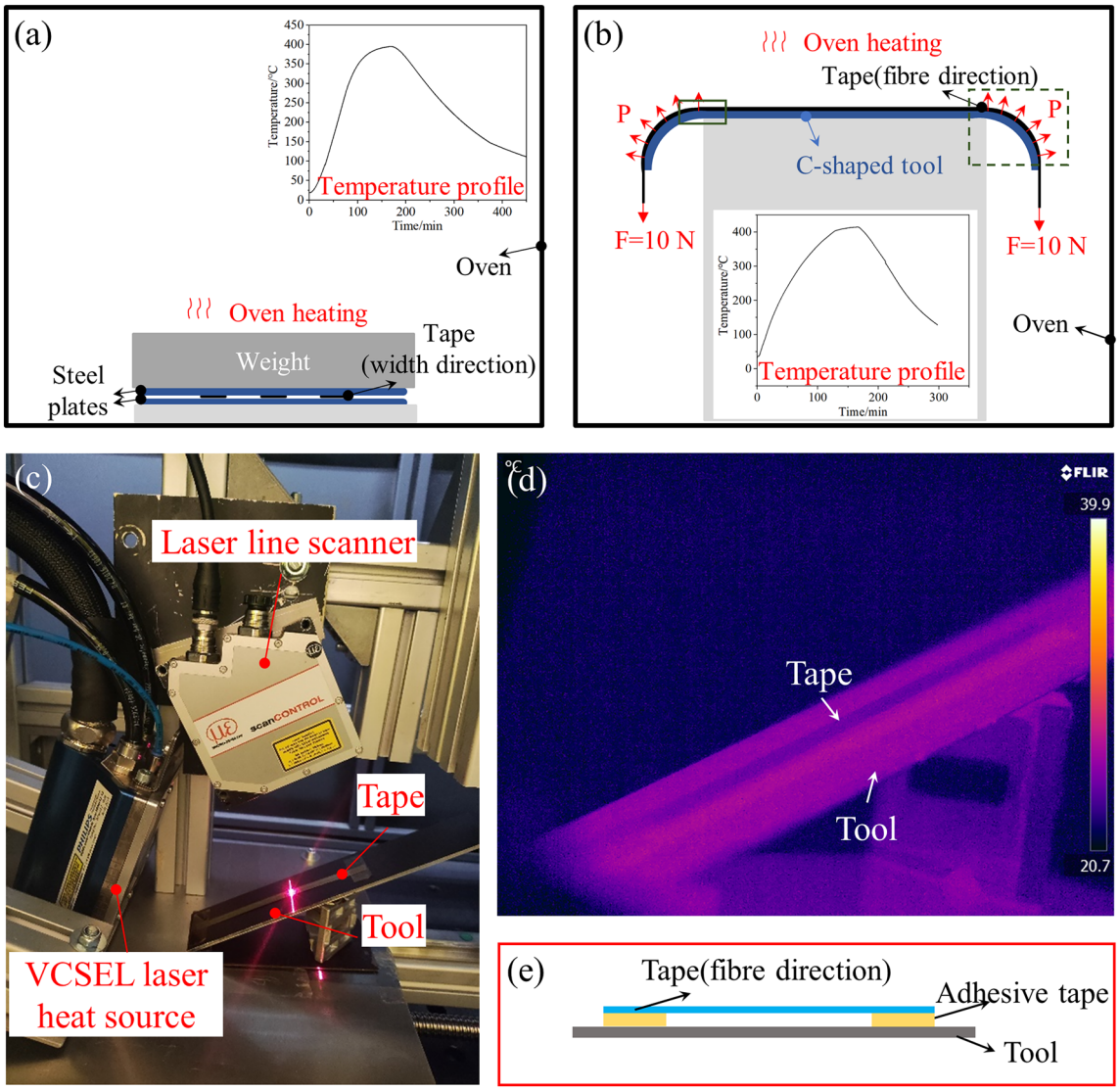

FIGURE 1 | Experimental setups: prepare (a) NS tape; (b) FS tape, (c) laser deconsolidation with VCSEL laser heat source, laser line scanner, tool, and thermal camera (example of the thermal image shown in (d)), and (e) placement of the CF/PEEK tape in the laser deconsolidation experiment.

above the tool by using adhesive tapes on both ends to make sure of complete separation of tape surface profiles from the tool (Figure 1e).

2.3 | Characterization

Deconsolidation was characterized through (1) the deformation along the width of the tape (quantified by arc-length width), (2) thickness, (3) intralaminar voids, (4) voids near surfaces, (5) fiber content through thickness, and (6) surface roughness.

2.3.1 | Arc-Length Width

As depicted in Figure 2a, the arc-length width is regarded as the actual tape width (for tapes with waviness), which is larger than the straight width (i.e., the width in the horizontal direction between the start and end of the tape) and was calculated from the surface profiles recorded by LLS. First, the high-frequency components in these surface profiles were filtered using the low-pass function in MATLAB. This function can remove the surface roughness information, retaining only the waviness of the tapes to calculate the arc-length width. The surface roughness of tapes after laser deconsolidation is in the range of 2–10 μm (measured by LSCM), corresponding to a cut-off length of 2500 μm [20]. Therefore, the passband frequency was set to 400 Hz to remove the influence of surface roughness. In Figure 2a, the filtered surface profile (after cooling) is compared with the waviness extracted from the cross-sectional micrograph at the same location, which is a spline curve along the center of the tape thickness direction. This comparison shows good consistency, demonstrating the effectiveness of filtering and using surface profiles to calculate arc-length width.

2.3.2 | Surface Roughness

The LSCM was utilized to measure the arithmetic mean deviation of surface roughness (Ra). Tapes for measuring surface roughness were cut into small pieces along the fiber direction, and four images (×10 magnification) of the tape surface were

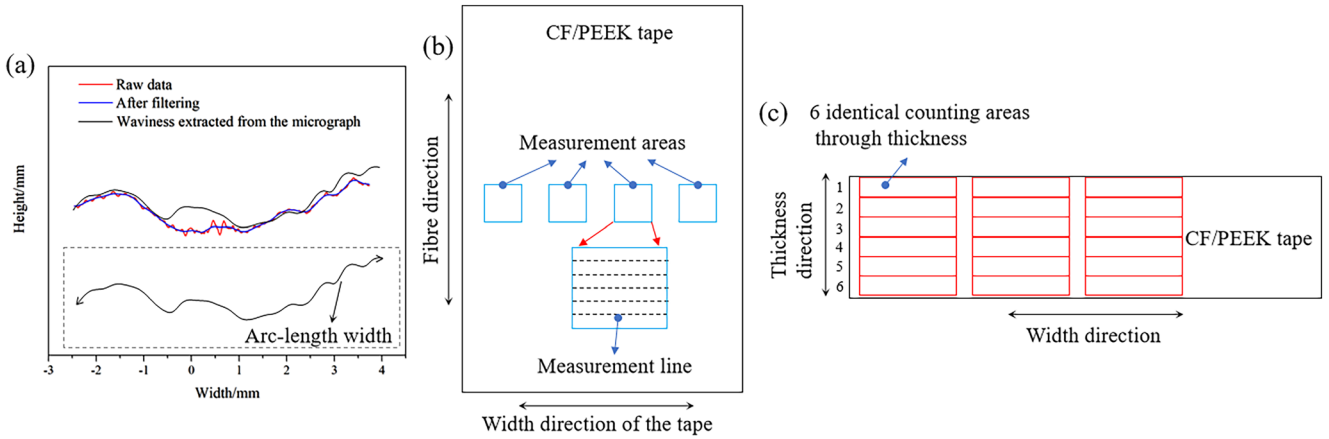

FIGURE 2 | Measurement methods for (a) the surface profile measured by LLS with (blue curve) and without (red curve) filtering, compared to the waviness (black curve) drawn from the microstructure. Dashed box illustrates the definition of arc-length width. (b) Surface roughness using LSCM. Four bule boxes represent the measurement areas at 20%, 40%, 60%, and 80% along the width of the tape. (c) Fiber content across tape thickness by counting fibers in each counting area.

uniformly captured along the whole width of each tape at a similar location as the cross-sectional micrographs. The Ra value for each sample was calculated using five lines in each image (see Figure 2b), and the average Ra value is based on measurements obtained from three different samples subjected to the same heat treatment.

2.3.3 | Microstructural Observation

Tapes after laser deconsolidation were cut near the measurement line of the LLS for cross-sectional micrographs, and other samples were cut in the middle of the tape. Thickness, voids and fiber content through thickness were analyzed through micrographs captured by an Olympus laser scanning confocal microscope (LSCM). The fiber content through thickness was measured by dividing the cross-sectional micrograph of the tape into six identical areas along the thickness direction. Three columns per width were used to obtain an average value. The fiber content was determined by counting the number of fibers in each area. Figure 2c shows the measurement method for fiber content through the thickness.

3 | Results and Discussion

3.1 | Characteristics of Tapes With Various Residual Stress Levels

Figure 3 shows cross-sections of FMS tape, FS tape, and NS tapes prior to deconsolidation. It can be seen in Figure 3a that FMS tape has a relatively uniform fiber/matrix distribution and is nearly void-free. In Figure 3b, the microstructure of the FS tape is presented. Due to the applied tape tension and pressure (0.45 bar) from the C-shaped tool, fibers are compacted toward the tool side, causing a flat tape surface at the tool side, and on the opposite side pools of matrix-rich areas and a nonuniform thickness due to the absence of pressure on the top surface of the tape.

The effect of various consolidation pressures can be seen in the cross-sections of NS tapes, as illustrated in Figure 3c–f, and the surface roughness Ra of the tapes is shown in Figure 3g. When the applied pressure is higher than or equal to 0.4 bar, NS tapes seem well consolidated in the oven: exhibiting a void-free structure and a matrix layer on the surfaces, and a low surface roughness Ra. Therefore, 0.4 bar is determined to be the minimum pressure required during oven consolidation in this work.

3.2 | Microstructure of Deconsolidated Tapes

3.2.1 | Oven Deconsolidation

Cross-sections of FMS-ODC (FMS tape after oven deconsolidation—ODC), FS-ODC, and NS-ODC (NS tapes consolidated at 0.4 bar) tapes are shown in Figure 4. Figure 4a shows that there is significant deformation along the width of the FMS tape after oven deconsolidation. From the high magnification microstructure in Figure 4b, it is observed that the FMS-ODC tape exhibits no intralaminar void, but there are some voids near the surfaces. Another important observation is the nonuniform thickness along the width of the tape. Locally, the thickness can increase to almost 0.18 mm, which is significantly higher than the tape's initial thickness (0.14 mm). All these phenomena, voids, deformation along the tape width, change in thickness are characterized as deconsolidation behavior. Figure 4c–f are cross-sections of the FS-ODC tape and NS-ODC tape, showing less pronounced deconsolidation behavior. For the FS-ODC tape (Figure 4d), the matrix-rich areas on the opposite side of the tool have diminished possibly due to the migration of fibers into these areas, and some voids are noticeable near that surface.

3.2.2 | Laser Deconsolidation

3.2.2.1 | Microstructures of Laser Deconsolidated (LDC) Tapes. FMS-LDC, FS-LDC, and NS-LDC (consolidated at 0.4 bar) tapes are shown in Figure 5. The FMS-LDC tape shows deformation along the width and also nonuniform thickness (Figure 5a,b), while the FS-LDC tape and NS-LDC tape remain

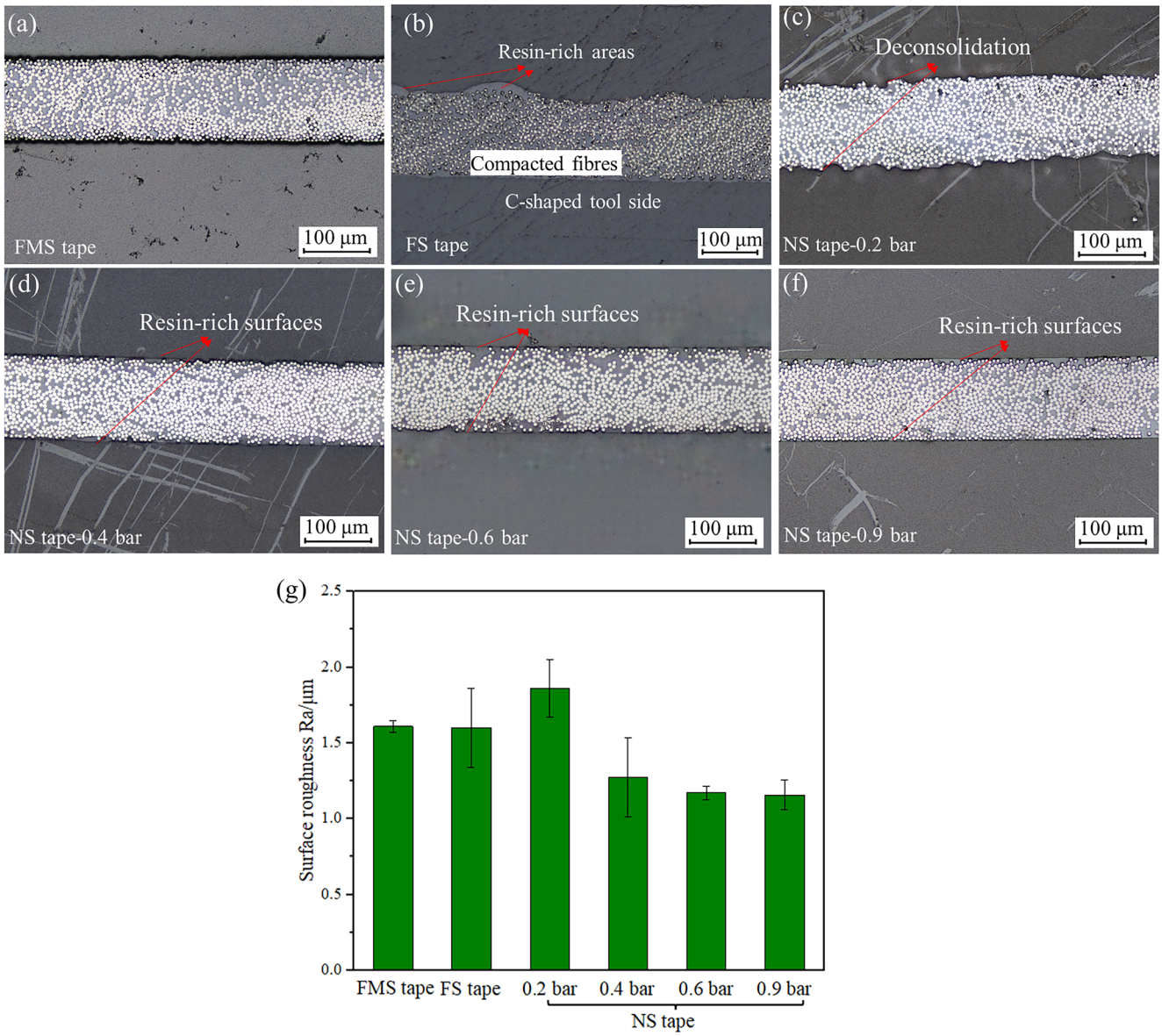

FIGURE 3 | Microstructural characteristics of (a) FMS tape; (b) FS tape; NS tapes prepared under different oven consolidation pressures of (c) 0.2 bar, (d) 0.4 bar, (e) 0.6 bar, and (f) 0.9 bar. (g) Measured surface roughness Ra of all groups of tapes.

relatively flat (Figure 5c,e). Figure 5b shows intralaminar voids in the FMS-LDC tape, showing a different deconsolidation behavior compared to oven deconsolidation (Figure 4b). The FS-LDC tape and NS-LDC tape show the same microstructural characteristics as the FS-ODC and NS-ODC tapes.

3.2.3 | Comparison of Deconsolidation Behavior

Several deconsolidation phenomena have been observed in the oven and laser deconsolidation experiments, shown in Figures 3–5. These phenomena are listed in Table 3 to compare deconsolidation behaviors. Deconsolidation phenomena, such as waviness and increased thickness, mostly happen when residual stress from the tape manufacturing process is present (FMS tape), indicating that residual stress seems to play an important role in their occurrence. The same holds true for intralaminar voids. These are observed only for the FMS tapes and only for the laser deconsolidation experiments, indicating that the formation of intralaminar voids is also dependent on the heating method. It is interesting to note that voids near the surface occur in all tapes with fiber residual stress (FS tape and FMS tape), indicating the influence of fiber stress on the occurrence of this type of void.

The surface roughness of the tapes is increased in all deconsolidation experiments. The surface roughness of FMS-LDC tape is significantly higher than that of FMS-ODC tape, and the surface roughness of FMS tape after deconsolidation is higher than that of NS tape and FS tape after deconsolidation. This also indicates that the matrix residual stress in the tapes and the heating method can change the deformation behavior significantly.

3.3 | Deformation Along the Width of the Tape

In Figure 6, the tape surface profile is coupled with the tape surface temperature (extracted at the center position of the LLS

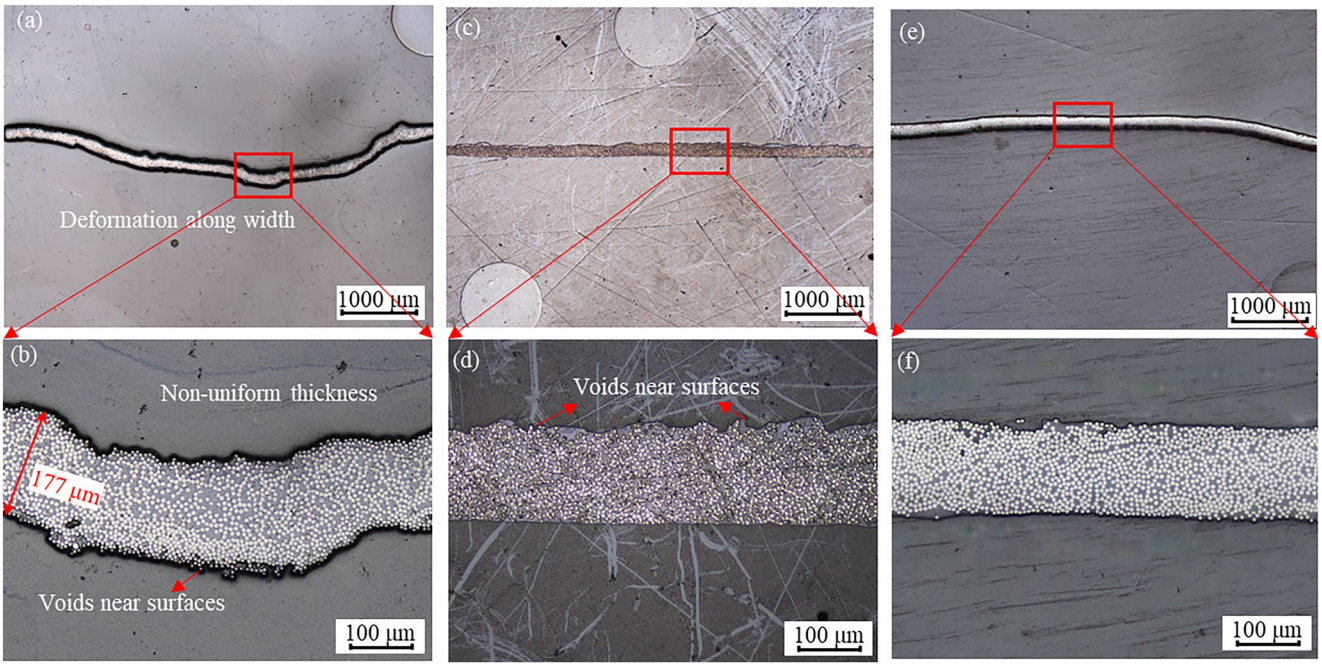

FIGURE 4 | Cross-sections of (a and b) FMS-ODC tape; (c and d) FS-ODC tape; and (e and f) NS-ODC tape (0.4 bar).

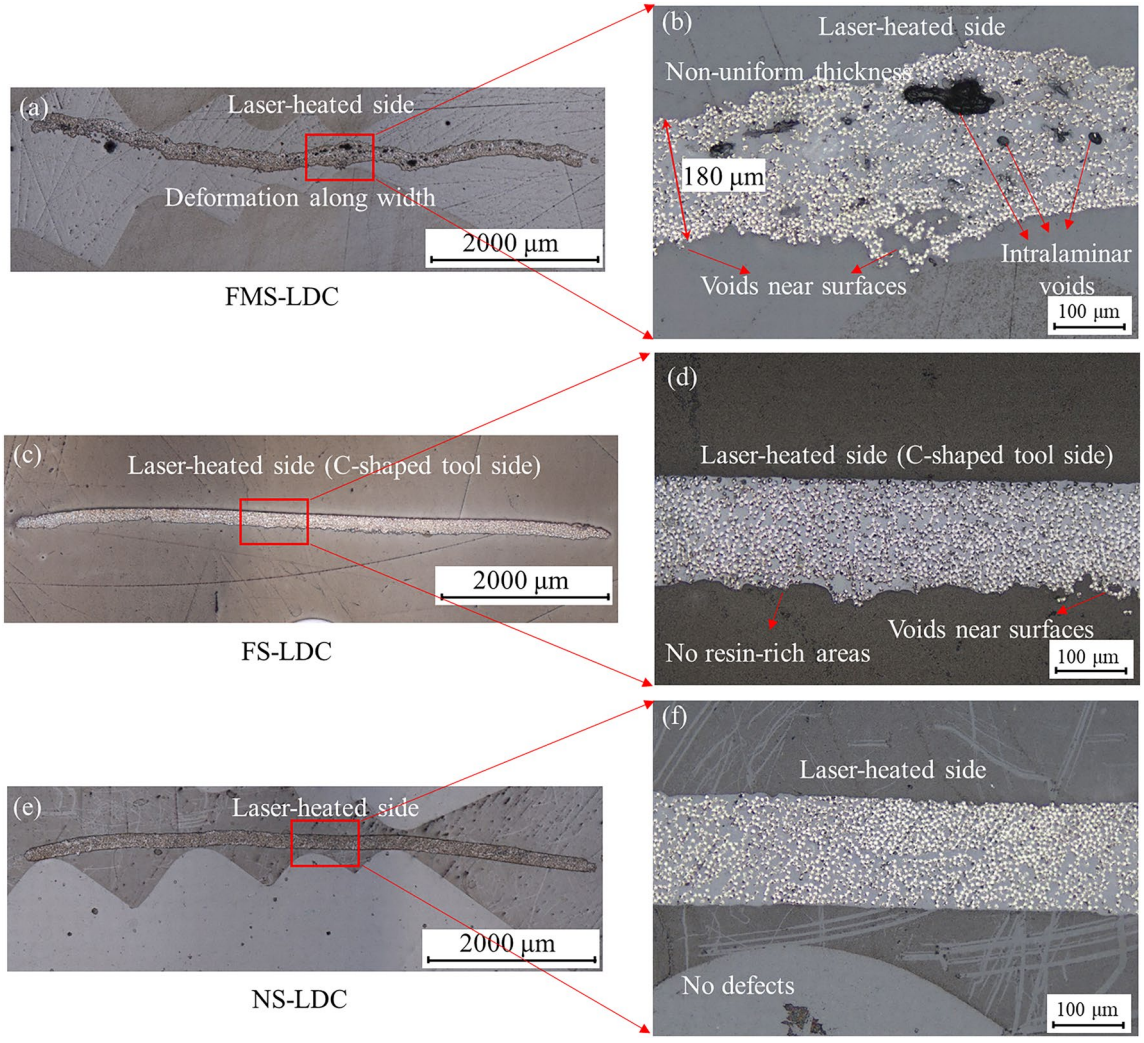

FIGURE 5 | Cross-sections of tapes after laser deconsolidation (LDC) (a and b) FMS-LDC tape, (c and d) FS-LDC tape, and (e and f) NS-LDC tape (0.4 bar).

TABLE 3 | Comparison of deconsolidation behavior ("+" means it occurs, "0" means it is not observed).

Tapes		FMS-ODC	FMS-LDC	FS-ODC	FS-LDC	NS-ODC	NS-LDC
Deformation along the width		+	+	0	0	+	0
Nonuniform thickness		+	+	0	0	0	0
Intralaminar voids		0	+	0	0	0	0
Voids near surfaces		+	+	+	+	0	0
Surface roughness Ra (μm)	Before deconsolidation	1.61 ± 0.04		1.84 ± 0.28		1.27 ± 0.26	
	After deconsolidation	3.15 ± 0.29	4.62 ± 0.73	1.98 ± 0.05	2.28 ± 0.30	2.72 ± 0.19	1.75 ± 0.15

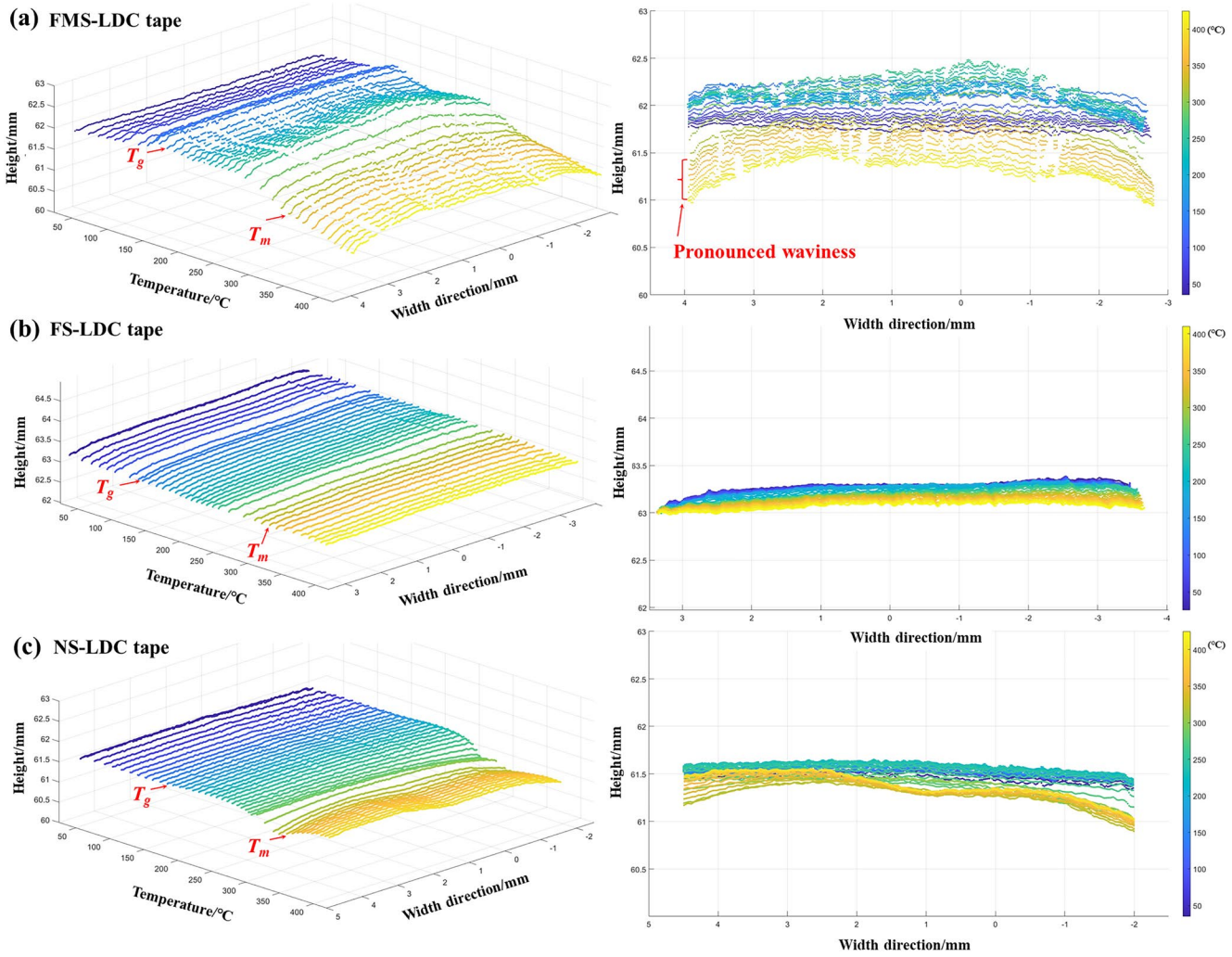

FIGURE 6 | Surface profiles (a) FMS-LDC tape, (b) FS-LDC tape, and (c) NS-LDC tape during laser deconsolidation. The different colors are used to clearly illustrate the changes in the tapes with temperature variation.

measurement line) during laser heating. The surface profiles are displayed every 0.02 s (50 Hz) to obtain surface profiles–temperature curves, driven by the sampling frequency of the LWIR camera (50 Hz), which shows that deformation along the width of the tape occurs during laser heating. Due to the gap between the tape and the tool, the overall height shows a decrease because of the sagging of the tapes in the length direction.

The deformation maps along the tape width from the top view and temperature maps are displayed in Figure 7. The left three figures in Figure 7 show that all three groups of tapes have continuous shrinkage along the width direction during the cooling phase. During laser heating, the FMS tape starts to deform at around T_g, and shows more pronounced waviness when the temperature reaches around T_m (Figures 6a and 7a), while NS and FS tapes have no noticeable deformation at T_g and only the NS

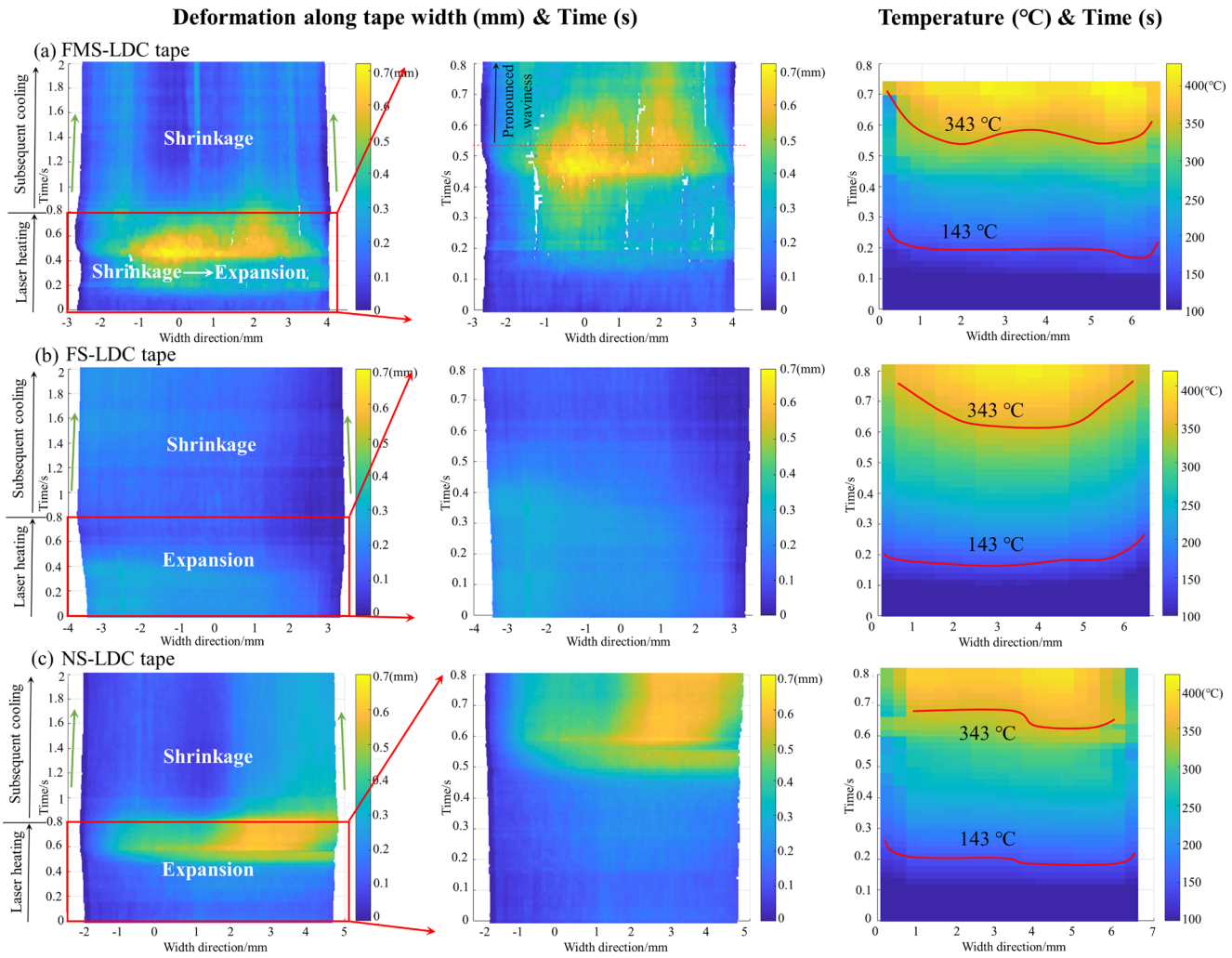

FIGURE 7 | Out of plane deformation maps along the width of tape (top view) and temperature maps during laser heating and subsequent cooling process over time of (a) FMS-LDC tape; (b) FS-LDC tape; and (c) NS-LDC tape.

tape shows slight deformation when the temperature reaches around T_m (Figures 6c and 7c). The in situ arc-length width, seen in Figure 8, was calculated based on the LLS data. During the entire heating time, the arc-length width of the FS-LDC tape and NS-LDC tape keeps increasing, dominated by thermal expansion [21], while the FMS-LDC tape decreases first and then increases, which shows a similar trend of change to that in Figure 7. The decrease of arc-length width of the FMS-LDC tape (the dashed box with a green background color) could be attributed to matrix cold crystallization [16], as more cold crystallization could cause a higher density and thus more compacted polymer chains.

Besides, the arc-length width of the FMS-LDC tape only increases until around 0.6 s (increased by 3.61%, close to the result 3.9% ± 0.7% in the published work of Çelik et al. [8]), approximately coinciding with the time when the pronounced waviness occurs (Figures 6a and 7a), while the FS-LDC tape and NS-LDC tape keep increasing until 0.8 s. Therefore, there seems to be another mechanism compensating for the thermal expansion of FMS tape during laser heating. It can most likely be attributed to the release of matrix residual stress in FMS tape [22], which is generated during the tape manufacturing process (as evidenced by the lack of such a phenomenon in the FS-LDC tape indicated by the red dotted curve in Figure 8b).

During the tape manufacturing process, molecular chains in the matrix would orient due to the pressure from the rotation bars and the tensile force along fiber bundles, causing them to be in a high potential energy state (unstable conformation) [23, 24]. But they do not have enough time to relax due to the high cooling rate of the process, causing matrix residual stress to be frozen in the tape. Besides, crystallization of the matrix during the cooling of the tape manufacturing process could also increase the residual stress because of the volume change when part of the matrix changes from amorphous state to crystalline state [16]. When the matrix is heated above its T_m, the residual stress within it can be released, causing the matrix in the tape to shrink [25], as shown in Figures 6 and 7 with no further expansion after reaching T_m.

3.4 | Fiber Decompaction and Void Formation

To understand the effect of the residual stress on fiber/matrix mobility and void formation, a study on the fiber distribution over the thickness of the FS tape and FS-LDC tape was conducted. Representative cross-sections were analyzed (see Figure 9a,b). It should be noted that the sixth counting area includes both tape materials and embedding epoxy resin, resulting in low fiber content.

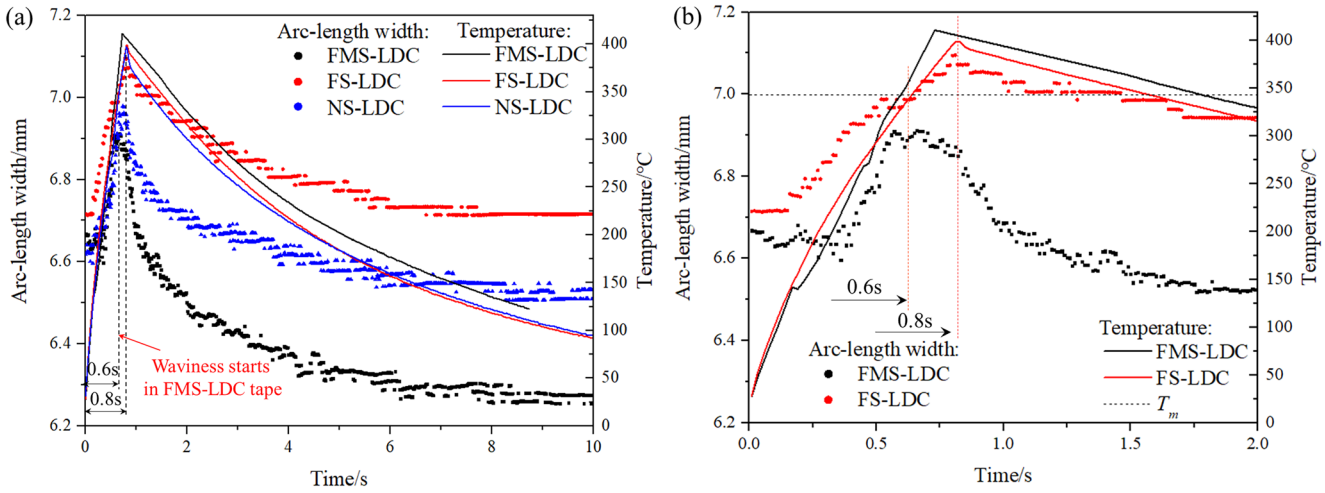

FIGURE 8 | Arc-length width and temperature profile of (a) FMS-LDC tape, FS-LDC tape, and NS-LDC tape during laser deconsolidation and (b) the first 2 s of FMS-LDC tape and FS-LDC tape.

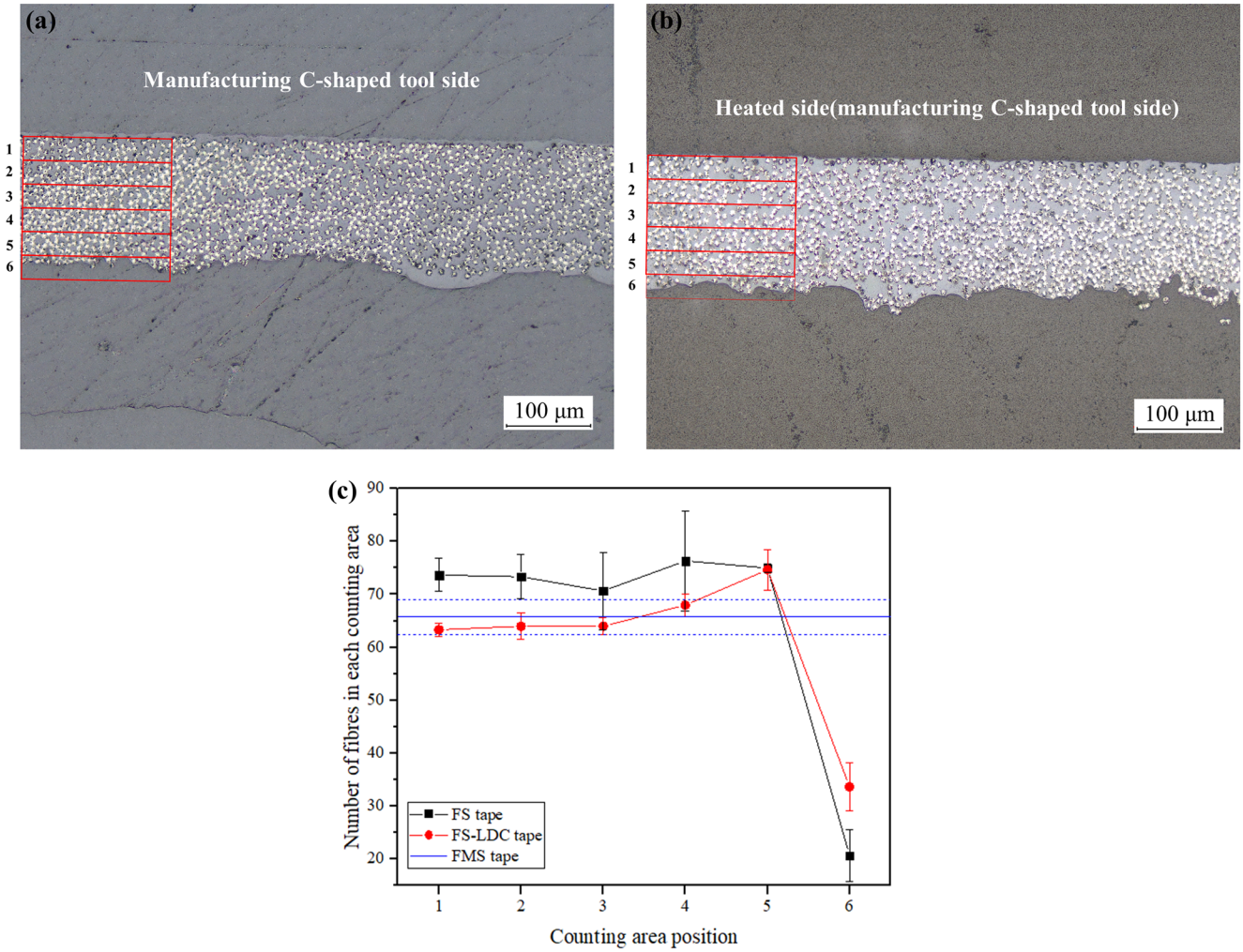

FIGURE 9 | Fiber distribution through the thickness of (a) FS tape; (b) FS-LDC tape; and (c) number of fibers in each counting area of FS tape, FS-LDC tape, and averaged fiber content in FMS tape.

For comparison, the average fiber content of the as-received FMS tape is also shown (using the same measurement method).

It is clear from Figure 9c that FS tape has more fibers near the heated side (counting area position 1) compared to FMS tape, and matrix-rich areas in the unheated side (counting area position 6). This difference could be attributed to the fiber compaction, which is caused by tape tension and the compaction force applied by the manufacturing tool. After laser deconsolidation, there are fibers in the previous matrix-rich areas and

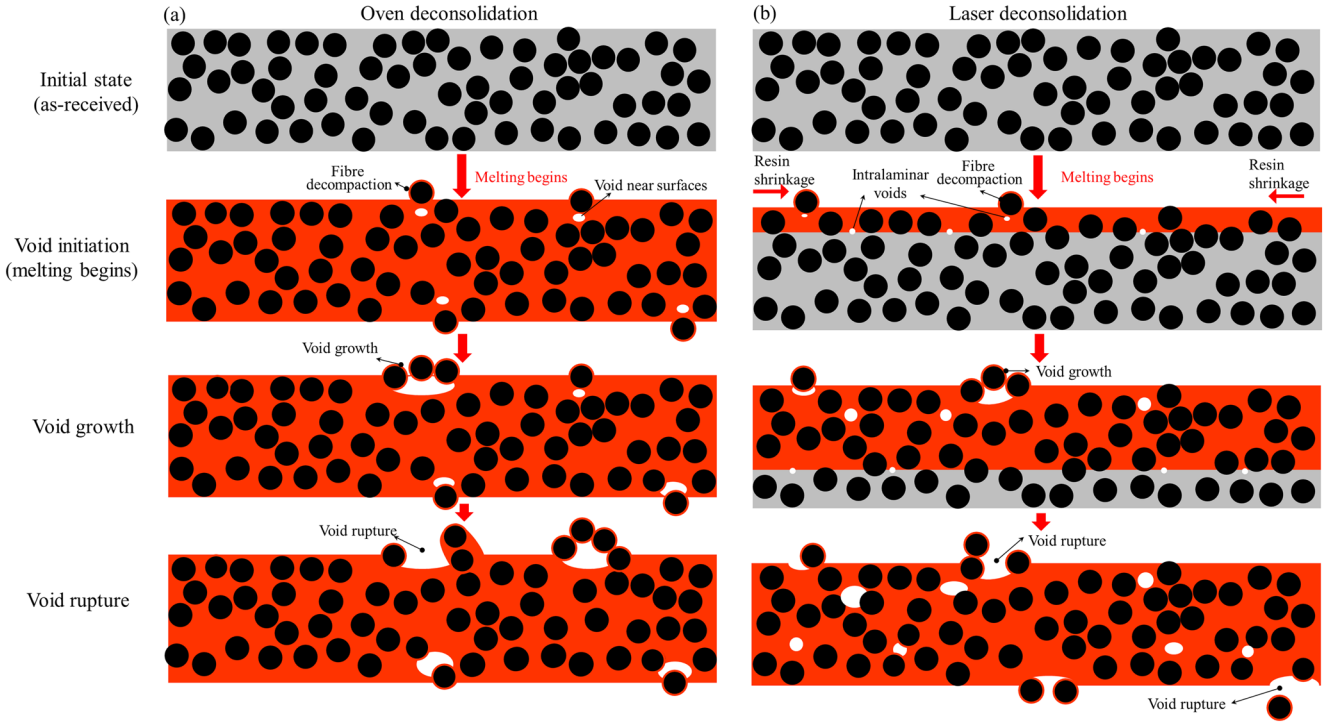

FIGURE 10 | Diagram of voids formation process in FMS tape during (a) oven deconsolidation and (b) laser deconsolidation.

more fibers present in the sixth counting area, which indicates that the fibers move to these areas during laser heating. The fiber content in the first four counting areas is decreased compared to before laser deconsolidation. This also means that fibers close to the laser-heated side seem to move to the unheated side (matrix-rich side). Since the fibers are stretched and compacted to the tool side during the FS tape manufacturing process, fibers' residual stress is stored in the form of elastic energy [26], which can be released by heating the tape above T_m. The relaxation of fibers' residual stress results in the movement of fibers from the tool side (heated side during laser heating experiments) to the other side (unheated side). Since there are only voids near the surface in FS-LDC tape, it seems to indicate that this type of voids is caused by fiber decompaction. Furthermore, as the FS-LDC tape has no intralaminar voids and remains flat, it indicates that it is the release of matrix residual stress that causes intralaminar voids, nonuniform thickness and deformation along the width in FMS-LDC tape (Figure 5a,b) rather than fibers' residual stress/movement.

Based on the results, the void formation process in the FMS-ODC tape and the FMS-LDC tape could be hypothesized as follows: During oven deconsolidation (Figure 10a), the compacted fibers in the FMS tape (compacted during the tape manufacturing process) near the tape surfaces start decompaction and tend to come out of the surfaces when the tape is heated upon T_m [8], causing the initiation of voids near the surfaces; voids keep growing when being heated to the maximum temperature; some of these voids rupture when they reach a critical size, as the surface tension and fluid viscosity of the matrix are unable to withstand their further growth [27]. This void formation process and phenomenon is in good agreement with the work of Amedewovo [28].

During laser deconsolidation (Figure 10b), the upper portion of the tape is first heated above T_m because of the temperature gradient across its thickness [29–31], which makes it possible for the release of matrix residual stress in this portion; significant deformation along the width of this melted part (shrinkage) as shown in Figure 5a,b, could lead to the initiation of voids at the melted and unmelted interfaces [32], which grow with the increase of temperature; fiber decompaction near surfaces also results in the type of voids near surfaces, similar to the process that occurred in oven deconsolidation; as the heating process progresses, matrix in the lower portion of the tape is melted, leading to the occurrence of more intralaminar voids. Therefore, for FMS-LDC tape, there are more and larger intralaminar voids near the laser-heated side. The void formation behavior during laser deconsolidation is consistent with the reported studies [33–35], where FMS-LDC tape exhibited voids on both surfaces and more intralaminar voids near the laser-heated side in matrix-rich areas.

4 | Conclusions

This study revealed pronounced effects of tape residual stress states and heating methods on the deconsolidation behavior of CF/TP tapes during the LAFP heating phase. Comparative analysis of three tape groups demonstrated that matrix residual stress in as-received tapes serves as the primary driver of deconsolidation during laser heating. Specifically, matrix stress release predominantly causes deformation along width and nonuniform thickness, and intralaminar void formation. Voids near surfaces observed in tapes with both fibers and matrix residual stresses as well as tapes with only fibers' residual stress were attributed to fiber decompaction. Laser-deconsolidated tapes exhibited more severe deconsolidation than oven-treated counterparts, particularly

in intralaminar voids. These voids seem to initiate through two mechanisms: (1) through-thickness temperature gradients during laser heating and (2) tensile stresses imposed by the unmelted matrix in the tape's lower part on the melted upper matrix.

The findings point toward producing as-received tapes with lower matrix residual stress to mitigate deconsolidation behavior. However, matrix and fiber residual stresses in the as-received tape cause different deconsolidation phenomena, such as the deformation along the width of the tape and voids near surfaces respectively. Future work should investigate which deconsolidation mechanism most critically affects intimate contact development. The laser heating rate used in this work is representative for in situ consolidation processes with AFP. When higher lay-up speeds and associated higher heating rates are to be used, their influence on the deconsolidation behavior also will be studied further.

Author Contributions

Qiuyu Miao: investigation, methodology, visualization, formal analysis, validation, writing – original draft, funding acquisition. **Daniël Peeters:** methodology, writing – review and editing, supervision. **Dongjiang Wu:** writing – review and editing, supervision. **Julie Teuwen:** methodology, writing – review and editing, supervision.

Acknowledgments

The authors gratefully acknowledge the financial support of the Program of China Scholarship Council (No. 202206060061).

Funding

This work was supported by the Program of China Scholarship Council (202206060061).

Conflicts of Interest

The authors declare no conflicts of interest.

Data Availability Statement

The data that support the findings of this study are available from the corresponding author upon reasonable request.

References

1. P. H. Li, Z. Y. Han, Y. M. Tong, Z. G. Cai, and S. Z. Sun, "Multi-Objective Optimization of Laser Heat Flux Distribution Considering Interlaminar Shear Strength and Warping in Laser-Assisted Automated Fiber Placement," *Polymer Composites* 46, no. S3 (2025): 29964, https://doi.org/10.1002/pc.29964.

2. C. C. Sun, R. Gergely, D. A. Okonski, and J. Y. Min, "Experimental and Numerical Investigations on Thermoforming of Thermoplastic Prepregs of Glass Fiber Reinforced Nylon 6," *Journal of Materials Processing Technology* 295 (2021): 117161, https://doi.org/10.1016/j.jmatprotec.2021.117161.

3. N. Koutras, J. Amirdine, N. Boyard, I. F. Villegas, and R. Benedictus, "Characterisation of Crystallinity at the Interface of Ultrasonically Welded Carbon Fibre PPS Joints," *Composites Part A: Applied Science and Manufacturing* 125 (2019): 105574, https://doi.org/10.1016/j.compositesa.2019.105574.

4. H. Nishida, V. Carvelli, T. Fujii, and K. Okubo, "Thermoplastic vs. Thermoset Epoxy Carbon Textile Composites," *IOP Conference Series: Materials Science and Engineering* 406 (2018): 12043, https://doi.org/10.1088/1757-899x/406/1/012043.

5. V. Donadei, F. Lionetto, M. Wielandt, A. Offringa, and A. Maffezzoli, "Effects of Blank Quality on Press-Formed PEKK/Carbon Composite Parts," *Materials* 11 (2018): 1063, https://doi.org/10.3390/ma11071063.

6. L. Ye, M. Lu, and Y. W. Mai, "Thermal De-Consolidation of Thermoplastic Matrix Composites—I. Growth of Voids," *Composites Science and Technology* 62 (2002): 2121–2130, https://doi.org/10.1016/S0266-3538(02)00144-6.

7. D. Saenz-Castillo, M. I. Martín, S. Calvo, F. Rodriguez-Lence, and A. Güemes, "Effect of Processing Parameters and Void Content on Mechanical Properties and NDI of Thermoplastic Composites," *Composites Part A: Applied Science and Manufacturing* 121 (2019): 308–320, https://doi.org/10.1016/j.compositesa.2019.03.035.

8. O. Çelik, A. Choudhary, D. Peeters, J. Teuwen, and C. Dransfeld, "Deconsolidation of Thermoplastic Prepreg Tapes During Rapid Laser Heating," *Composites Part A-Applied Science and Manufacturing* 149 (2021): 106575, https://doi.org/10.1016/j.compositesa.2021.106575.

9. T. Kok, *The Role of Heating Phase on the Consolidation Quality in Laser Assisted Fibre Placement* (University of Twente, 2018).

10. O. Çelik, D. Peeters, C. Dransfeld, and J. Teuwen, "Intimate Contact Development During Laser Assisted Fibre Placement: Microstructure and Effect of Process Parameters," *Composites Part A: Applied Science and Manufacturing* 134 (2020): 105888, https://doi.org/10.1016/j.compositesa.2020.105888.

11. T. K. Slange, L. L. Warnet, W. J. B. Grouve, and R. Akkerman, "Deconsolidation, of C/PEEK Blanks: On the Role of Prepreg, Blank Manufacturing Method and Conditioning," *Composites Part A: Applied Science and Manufacturing* 113 (2018): 189–199, https://doi.org/10.1016/j.compositesa.2018.06.034.

12. L. Amedewovo, A. Levy, B. D. Plessix, et al., "A Methodology for Online Characterization of the Deconsolidation of Fibre-Reinforced Thermoplastic Composite Laminates," *Composites Part A-Applied Science and Manufacturing* 167 (2023): 107412, https://doi.org/10.1016/j.compositesa.2022.107412.

13. T. K. Slange, L. L. Warnet, W. J. B. Grouve, and R. Akkerman, "Influence of Prepreg Characteristics on Stamp Consolidation," *AIP Conference Proceedings* 1896 (2017): 30034.

14. R. Marissen, L. D. Drift, and J. Sterk, "Technology for Rapid Impregnation of Fibre Bundles With a Molten Thermoplastic Polymer," *Composites Science and Technology* 60, no. 10 (2000): 2029–2034, https://doi.org/10.1016/S0266-3538(00)00122-6.

15. W. Jiang, C. Chen, Z. Chen, Z. Huang, and H. Zhou, "Effect of Crystallinity on Optical Properties of PEEK Prepreg Tapes for Laser-Assisted Automated Fibre Placement," *Composition & Communication* 38 (2023): 101490, https://doi.org/10.1016/j.coco.2022.101490.

16. M. Golzar, J. Sinke, and M. Abouhamzeh, "Novel Thermomechanical Characterization for Shrinkage Evolution of Unidirectional Semi-Crystalline Thermoplastic Prepregs (PPS/CF) in Melt, Rubbery and Glassy States," *Composites Part A-Applied Science and Manufacturing* 156 (2022): 106879, https://doi.org/10.1016/j.compositesa.2022.106879.

17. C. Filiou, C. Galiotis, and D. N. Batchelder, "Residual Stress Distribution in Carbon Fibre/Thermoplastic Matrix Pre-Impregnated Composite Tapes," *Composites* 23, no. 1 (1992): 28–38, https://doi.org/10.1016/0010-4361(92)90283-Z.

18. Toray Cetex TC1200, PEEK Product Data Sheet, https://www.toraytac.com/product-explorer/products/ovl4/Toray-Cetex-TC1200.

19. L. Zhao, S. C. Mantell, D. Cohen, and R. McPeak, "Finite Element Modeling of the Filament Winding Process," *Composite Structures* 52 (2001): 499–510, https://doi.org/10.1016/S0263-8223(01)00039-3.

20. BS EN ISO 4288-1998, *Geometric Product Specification (GPS)—Surface Texture—Profile Method: Rules and Procedures for the Assessment of Surface Texture* (1998).

21. J. A. Barnes, "Thermal Expansion Behaviour of Thermoplastic Composites," *Journal of Materials Science* 28 (1993): 4974–4982, https://doi.org/10.1007/BF00361164.

22. C. Hopmann, E. Wilms, C. Beste, D. Schneider, K. Fischer, and S. Stender, "Investigation of the Influence of Melt-Impregnation Parameters on the Morphology of Thermoplastic UD-Tapes and a Method for Quantifying the Same," *Journal of Thermoplastic Composite Materials* 34, no. 9 (2019): 1299–1312, https://doi.org/10.1177/0892705719864624.

23. S. Zhan, H. Xu, H. Duan, et al., "Molecular Dynamics Simulation of Microscopic Friction Mechanisms of Amorphous Polyethylene," *Soft Matter* 15, no. 43 (2019): 8827–8839, https://doi.org/10.1039/C9SM01533G.

24. J. Y. Chung, T. Q. Chastek, M. J. Fasolka, H. W. Ro, and C. M. Stafford, "Quantifying Residual Stress in Nanoscale Thin Polymer Films via Surface Wrinkling," *ACS Nano* 3, no. 4 (2009): 844–852, https://doi.org/10.1021/nn800853y.

25. M. Greisel, J. Jäger, J. Moosburger-Will, M. G. R. Sause, W. M. Mueller, and S. Horn, "Influence of Residual Thermal Stress in Carbon Fiber-Reinforced Thermoplastic Composites on Interfacial Fracture Toughness Evaluated by Cyclic Single-Fiber Push-Out Tests," *Composites Part A, Applied Science and Manufacturing* 66 (2014): 117–127, https://doi.org/10.1016/j.compositesa.2014.07.010.

26. M. Lu, L. Ye, and Y. Mai, "Thermal De-Consolidation of Thermoplastic Matrix Composites-II. "Migration" of Voids and "Re-Consolidation"," *Composites Science and Technology* 64, no. 2 (2004): 191–202, https://doi.org/10.1016/S0266-3538(03)00233-1.

27. M. A. Khan, P. Mitschang, and R. Schledjewski, "Tracing the Void Content Development and Identification of Its Effecting Parameters During In Situ Consolidation of Thermoplastic Tape Material," *Polymers and Polymer Composites* 18, no. 1 (2010): 1–15, https://doi.org/10.1177/096739111001800101.

28. A. M. Kollmannsberger, *Heating Characteristics Offixed Focus Laser Assisted Thermoplastic-Automated Fibre Placement of 2D and 3D Parts* (Technical University of Munich, 2019).

29. Y. Ding, G. Feng, D. H. H. Hoffmann, et al., "Meso-Scale Simulation of Temperature Field in Composite Materials Under Laser Irradiation," in *Fourth International Symposium on Laser Interaction With Matter* (Proc. SPIE, 2017), 101730, https://doi.org/10.1117/12.2268338.

30. A. J. Toro, J. J. E. Teuwen, F. Tomás, and W. Finnegan, "The Role of Melting on Intimate Contact Development in Laser-Assisted Tape Placement of Carbon Fibre Reinforced Thermoplastic Composites," in *Proceedings of the 20th European Conference on Composite Materials: Composites Meet Sustainability*, vol. 2 (Composite Construction Laboratory, 2022), 242–249.

31. M. Ponçot, F. Addiego, and A. Dahoun, "True Intrinsic Mechanical Behaviour of Semi-Crystalline and Amorphous Polymers: Influences of Volume Deformation and Cavities Shape," *International Journal of Plasticity* 40 (2013): 126–139, https://doi.org/10.1016/j.ijplas.2012.07.007.

32. A. Choudhary, *Thermal Deconsolidation of Thermoplastic Prepreg Tapes During Laser-Assisted Fibre Placement* (Delft University of Technology, 2019).

33. Y. M. Blommert, *Deconsolidation of Thermoplastic Prepreg Tapes During the Heating Phase of LAFP* (Delft University of Technology, 2022).

34. O. Çelik, S. M. A. Hosseini, I. Baran, et al., "The Influence of Inter-Laminar Thermal Contact Resistance on the Cooling of Material During Laser Assisted Fibre Placement," *Composites Part A: Applied Science and Manufacturing* 145 (2021): 106367, https://doi.org/10.1016/j.compositesa.2021.106367.

35. L. Amedewovo, L. Orgéas, B. D. Plessix, N. Lefevre, A. Levy, and S. Corre, "Deconsolidation of Carbon Fibre-Reinforced PEKK Laminates: 3D Real-Time In Situ Observation With Synchrotron X-Ray Microtomography," *Composites Part A: Applied Science and Manufacturing* 177 (2024): 107917, https://doi.org/10.1016/j.compositesa.2023.107917.